NASA TECHNICAL REPORT

NASA TR R-166

NASA TR R-166

ELASTIC CONSTANTS FOR BENDING AND TWISTING OF CORRUGATION-STIFFENED PANELS

by W. Jefferson Stroud

Langley Research Center

Langley Station, Hampton, Va.

NATIONAL AERONAUTICS AND SPACE ADMINISTRATION • WASHINGTON, D. C. • DECEMBER 1963

ELASTIC CONSTANTS FOR BENDING AND TWISTING OF CORRUGATION-STIFFENED PANELS

By W. Jefferson Stroud

Langley Research Center
Langley Station, Hampton, Va.

NATIONAL AERONAUTICS AND SPACE ADMINISTRATION

For sale by the Office of Technical Services, Department of Commerce,
Washington, D.C. 20230 -- Price $1.25

ELASTIC CONSTANTS FOR BENDING AND TWISTING OF CORRUGATION-STIFFENED PANELS*

By W. Jefferson Stroud

SUMMARY

Theoretical formulas for five orthotropic elastic constants associated with pure bending and pure twist are presented for a corrugation-stiffened panel. The constants are the bending stiffnesses parallel to and normal to the corrugation direction, the twisting stiffness, and the Poisson's ratios associated with bending. The formulas are given in terms of the dimensions of the corrugation pattern for the general case of different corrugation and cover-plate materials. Bending stiffnesses measured on panels with three different corrugation patterns, and twisting stiffnesses measured on panels with two different patterns, compare favorably with the theoretical results.

INTRODUCTION

A type of structural panel used in the skin of the X-15 and having potential use for the skin of hypersonic aircraft and reentry vehicles consists of a corrugated metal plate attached to one side of a flat metal plate. Such a panel may be thought of as a plate stiffened by corrugations and is referred to in this report as a corrugation-stiffened panel. This type of stiffened panel is easy to fabricate and for those applications where the primary load-carrying function requires a high bending stiffness in one direction, it provides an efficient use of the material. Its main disadvantage is that the bending stiffness in the other direction is extremely small. Thus it may be susceptible, in some applications, to undesirable effects such as panel flutter.

In order to predict the structural characteristics of a corrugation-stiffened panel (its panel-flutter characteristics as well as its load-carrying ability), information is needed about the elastic constants of the panel. These constants define the resistance of a loaded panel to deformation. As discussed

---

*Part of the information presented herein was included in a thesis entitled "The Bending and Twisting Stiffnesses of Corrugation Stiffened Panels" submitted in partial fulfillment of the requirements for the degree of Master of Science in Engineering Mechanics, Virginia Polytechnic Institute, Blacksburg, Virginia, June 1962.

in reference 1, in which corrugated-core sandwich panels are considered, the constants include two transverse shear stiffnesses D_{Q_x} and D_{Q_y}, two bending stiffnesses D_x and D_y, a twisting stiffness D_{xy}, two stretching moduli E_x and E_y, a shearing modulus G_{xy}, two Poisson's ratios μ_x and μ_y associated with bending, and two Poisson's ratios μ'_x and μ'_y associated with stretching.

In the present paper the five elastic constants associated with pure bending and pure twist, D_x, D_y, D_{xy}, μ_x, and μ_y, are considered. Formulas are given for these five constants in terms of the dimensions of the corrugation pattern for the general case of different corrugation and cover-plate materials. Theoretical values of D_x, D_y, and D_{xy} are compared with experimental values for three corrugation patterns. For each specimen tested, the cover-plate material was the same as the corrugation material.

SYMBOLS

A	area enclosed by corrugation cell
$a,b,d,e_1,e_2,g,i,j,k,n,p,r_1,r_2,\bar{y},\theta$	dimensions of corrugation pattern (see fig. 2)
c_1,c_2,c_3	constants in solution of differential equation in appendix D
D	plate stiffness per unit width, $\frac{Et^3}{12(1-\mu^2)}$, in-lb
D_x,D_y	bending stiffnesses per unit width of a beam cut from orthotropic panel in x- and y-directions, respectively, in-lb
D_{xy}	twisting stiffness of unit-width and unit-length element cut from orthotropic panel, with edges parallel to x- and y-axes, in-lb
D_y'	beam bending stiffness in y-direction per unit width for segment of panel of length 2b (defined in eq. (B19))
D_y''	beam bending stiffness in y-direction per unit width for segment of panel of length 2a (defined in eq. (B27))
E	Young's modulus, lb/sq in.
G	shear modulus, lb/sq in.
H	quantity associated with shape of corrugation (defined by eq. (B12))
I	moment of inertia per unit width, $in.^3$

$\bar{I}$	area moment of inertia per unit width of cross section, $in.^3$
$\bar{J}$	torsion constant per unit width of cross section, $in.^3$
K	curvature in x-direction
M	moment per unit width, in-lb/in.
M_x, M_y	resultant bending-moment intensities in x- and y-directions, respectively, in-lb/in.
M_{xy}	resultant twisting-moment intensity with regard to x- and y-directions, in-lb/in.
n	integer
P	in-plane load per unit width acting on corrugation and cover plate at weld line, lb/in. (see figs. 13 and 15)
r_y	radius of curvature in y-direction, in.
s	coordinate measured along center line of sheet making up corrugation cell, in.
t	thickness, in.
U	strain energy due to bending, in-lb
u, v, w_r	displacements in x-, ϕ-, and radial directions of middle surface of a cylinder, respectively
$v_1(\phi), w_1(\phi)$	functions arising from integrations (see eqs. (D9) and (D10), respectively)
w	displacement in z-direction, in.
X	quantity associated with shape of corrugation (defined by eq. (B14))
x	coordinate, measured parallel to corrugation direction, in.
y	coordinate, measured parallel to cover plate and perpendicular to corrugation direction, in.
z	coordinate, measured perpendicular to cover plate, in.
$\bar{z}$	distance from outer surface of cover plate to neutral axis of segment of length 2a, in.
$\gamma_{x\phi}$	shear strain, in./in.
δ	extension of elements

ϵ	strain, in./in.
$\bar{\theta}$	angular coordinate for elements BC and DE; from B to C for element BC, from D to E for element DE, radians (see fig. 13)
μ	Poisson's ratio of material
μ_x,μ_y	Poisson's ratios associated with curvature in y-direction caused by M_x loading and with curvature in x-direction caused by M_y loading, respectively
μ_{x1}	Poisson's ratio in x-direction for segment of panel of length 2b (defined by eq. (D52))
μ_{x2}	Poisson's ratio in x-direction for segment of panel of length 2a (defined by eq. (D55))
ξ	distance measured along element CD, in. (see figs. 13 and 15)
Σ	quantity associated with material and shape of corrugation (defined in eq. (D43))
σ	stress, lb/sq in.
ϕ	angular coordinate measured clockwise from the vertical, radians (see fig. 15)
Λ,Φ,Ω	quantities associated with shape of corrugation (defined in eqs. (D41) and (D49))

Subscripts:

c	refers to corrugation
exp	experimental
p	refers to plate to which corrugation is welded
th	theoretical
x	refers to x-direction
y	refers to y-direction
ξ	refers to ξ-direction
ϕ	refers to circumferential direction
1,2,. . . 5	refers to extensions in y-direction of elements AB,BC,. . . EF, respectively

THEORETICAL RESULTS

The bending and twisting elastic constants used herein are defined in the following pure-bending and pure-twisting relationships (see, for example, ref. 2):

$$M_x = -\frac{D_x}{1 - \mu_x\mu_y}\left(\frac{\partial^2 w}{\partial x^2} + \mu_y \frac{\partial^2 w}{\partial y^2}\right)$$

$$M_y = -\frac{D_y}{1 - \mu_x\mu_y}\left(\frac{\partial^2 w}{\partial y^2} + \mu_x \frac{\partial^2 w}{\partial x^2}\right)$$

$$M_{xy} = D_{xy} \frac{\partial^2 w}{\partial x\, \partial y}$$

The directions for M_x, M_y, and M_{xy} - and, consequently, the directions for D_x, D_y, and D_{xy} - are indicated in figure 1. The stiffnesses D_x, D_y, and D_{xy} are associated with the resultant moments M_x, M_y, and M_{xy}, respectively. When the transverse shear stiffness is assumed infinite, the differential equation for lateral deflections of an orthotropic panel consistent with these definitions of the elastic constants is

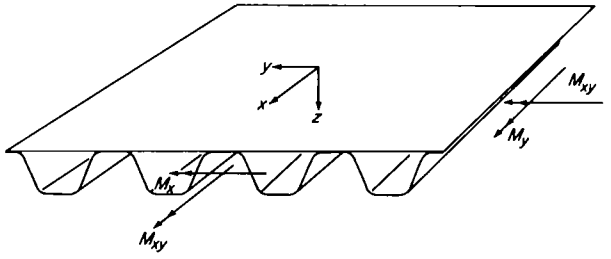

Figure 1.- Typical corrugation-stiffened panel.

$$\frac{D_x}{1-\mu_x\mu_y}\frac{\partial^4 w}{\partial x^4} + 2\left(D_{xy} + \frac{\mu_y D_x}{1-\mu_x\mu_y}\right)\frac{\partial^4 w}{\partial x^2 \partial y^2} + \frac{D_y}{1-\mu_x\mu_y}\frac{\partial^4 w}{\partial y^4} = q + N_x \frac{\partial^2 w}{\partial x^2} + N_y \frac{\partial^2 w}{\partial y^2} + 2N_{xy}\frac{\partial^2 w}{\partial x\, \partial y}$$

where

q lateral load, lb/sq in.

N_x, N_y intensities of resultant normal force acting in x- and y-directions, respectively, lb/in.

N_{xy} intensity of resultant shearing force in xy-plane, lb/in.

Derivations of theoretical expressions for the three stiffnesses D_x, D_y, and D_{xy} and the Poisson's ratios μ_x and μ_y for cross-section shapes of the type shown in figure 2 are outlined in appendixes A, B, C, and D for the general case in which the cover-plate material and corrugation material are different. For easy reference, results for the case in which the cover-sheet and corrugation material are the same are given by the following expressions:

For the bending stiffness in the x-direction:

$$D_x = E\bar{I} \tag{1}$$

where E is the Young's modulus of the panel material,

$$\bar{I} = \frac{2}{p}\left[\frac{(a+b)t_p^3}{12} + \left(\bar{y} - \frac{t_p}{2}\right)^2(a+b)t_p + \frac{(a+i)t_c^3}{12} + \left(e_1 + r_1\right)^2(a+i)t_c + t_c r_1^3\left(\frac{\theta}{2} + \frac{\sin 2\theta}{4}\right)\right.$$

$$+ 2t_c e_1 r_1^2 \sin\theta + e_1^2 r_1 \theta t_c + \frac{t_c}{12} k^3 \sin^2\theta + \frac{kt_c^3}{12}\cos^2\theta + \left(t_p + \frac{t_c}{2} + j + \frac{k}{2}\sin\theta - \bar{y}\right)^2 kt_c$$

$$\left. + t_c r_2^3\left(\frac{\theta}{2} + \frac{\sin 2\theta}{4}\right) + 2t_c e_2 r_2^2 \sin\theta + e_2^2 r_2 \theta t_c + \frac{gt_c^3}{12} + \left(e_2 + r_2\right)^2 t_c g\right] \tag{2}$$

and

$$\bar{y} = \frac{\left[\frac{t_p^2}{2}(b+a) + \left(t_p + \frac{t_c}{2}\right)(a+i)t_c + \left(t_p + \frac{t_c}{2} + r_1 - \frac{r_1 \sin\theta}{\theta}\right)r_1\theta t_c + \left(t_p + \frac{t_c}{2} + j + \frac{n-j}{2}\right)kt_c\right.}{t_p(b+a) + (a+i)t_c + r_1\theta t_c + kt_c + r_2\theta t_c + gt_c}$$

$$\left. + \left(t_p + \frac{t_c}{2} + d - r_2 + \frac{r_2 \sin\theta}{\theta}\right)r_2\theta t_c + \left(t_p + \frac{t_c}{2} + d\right)gt_c\right] \tag{3}$$

All the symbols on the right-hand sides of equations (2) and (3) are dimensions shown in figure 2.

In particular, note from figure 2 that

$$e_1 = \bar{y} - \left(r_1 + t_p + \frac{t_c}{2}\right) \tag{4}$$

$$e_2 = d - \left(r_1 + r_2 + e_1\right) \tag{5}$$

$$j = r_1(1 - \cos\theta) \tag{6}$$

$$n = d - r_2(1 - \cos\theta) \tag{7}$$

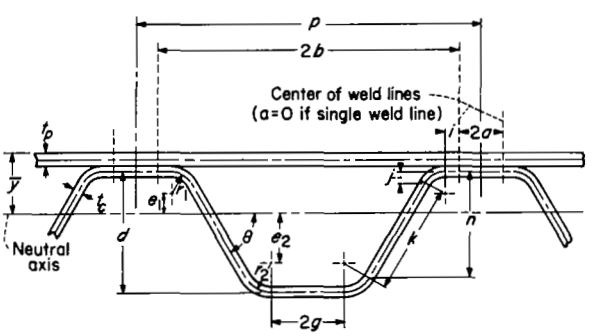

Figure 2.- Dimensions of corrugation cell.

Throughout this report, the subscript c refers to the corrugation and the subscript p refers to the plate to which the corrugation is attached.

For the bending stiffness in the y-direction:

$$D_y = \frac{a + b}{\frac{a}{D_y''} + \frac{b}{D_y'}} \tag{8}$$

where

$$D_y' = \left(\frac{bD_c}{X} + D_p\right)\left(1 - \mu_x\mu_y\right) \tag{9}$$

$$D_y'' = \frac{E\left(t_p + t_c\right)^3}{12\left(1 - \mu^2\right)}\left(1 - \mu_x\mu_y\right) \tag{10}$$

In equations (9) and (10), μ is the Poisson's ratio of the panel material,

$$D_c = \frac{Et_c^3}{12\left(1 - \mu^2\right)} \tag{11}$$

$$D_p = \frac{Et_p^3}{12\left(1 - \mu^2\right)} \tag{12}$$

and

$$X = i + \left(r_1 + r_2\right)\theta + k + g - H\left[r_1^2(\theta - \sin\theta) + jk + \frac{k^2}{2}\sin\theta + r_2\left(n\theta - r_2\theta\cos\theta + r_2\sin\theta\right) + gd\right] \tag{13}$$

where

$$H = \frac{r_1^2(\theta - \sin\theta) + jk + \frac{k^2}{2}\sin\theta + r_2\left(n\theta - r_2\theta\cos\theta + r_2\sin\theta\right) + gd}{\left[r_1^3\left(\frac{3\theta}{2} - 2\sin\theta + \frac{\sin 2\theta}{4}\right) + j^2k + jk^2\sin\theta + \frac{k^3}{3}\sin^2\theta + r_2n^2\theta - 2nr_2^2\theta\cos\theta + 2nr_2^2\sin\theta + \frac{r_2^3}{2}(3\theta - 3\sin\theta\cos\theta - 2\theta\sin^2\theta) + gd^2\right]} \tag{14}$$

The quantities μ_x and μ_y are defined subsequently but the product $\mu_x\mu_y$ is usually small compared with unity and can be neglected in the calculation of D_y' and D_y''.

For the twisting stiffness:

$$D_{xy} = \frac{G\bar{J}}{2} \tag{15}$$

where G is the shear modulus of the panel material and

$$\bar{J} = \frac{\frac{2}{p}\left\{b\left(t_c + t_p\right) + d\left[b + g - i + \left(r_2 - r_1\right)\tan\frac{\theta}{2}\right] + 2\left(r_1^2 - r_2^2\right)\tan\frac{\theta}{2} + \left(r_2^2 - r_1^2\right)\theta\right\}^2}{\frac{b}{t_p} + \frac{1}{t_c}\left[i + \theta\left(r_1 + r_2\right) + k + g\right]} \tag{16}$$

For Poisson's ratio associated with curvature in the y-direction caused by M_x loading:

$$\mu_x = \frac{b\mu_{x1} + a\mu}{b + a} \tag{17}$$

where

$$\mu_{x1} = \frac{-H\Sigma}{\frac{D_p}{D_c}X + b} \tag{18}$$

and

$$\Sigma = \mu\left\{i\left(e_1 + r_1\right) + r_1 e_1 \sin\theta + r_1^2 \sin\theta\cos\theta + \frac{\cot\theta}{2}\left[\left(e_1 + r_1\cos\theta\right)^2 - \left(e_2 + r_2\cos\theta\right)^2\right] - r_2 e_2 \sin\theta - r_2^2 \sin\theta\cos\theta - g\left(e_2 + r_2\right) - b\left(\bar{y} - \frac{t_p}{2}\right)\right\} \tag{19}$$

For Poisson's ratio associated with curvature in the x-direction caused by M_y loading, the following relationship, which can be derived from the theorem of reciprocity (ref. 3), is used:

$$\mu_y = \mu_x \frac{D_y}{D_x} \tag{20}$$

In the derivation of equations (1) and (15), the panel was considered to be made up of a series of cells or thin-walled tubes. In addition, for equation (15), the angle of twist of each corrugation element was considered to be equal to the angle of twist of the panel as a whole.

EXPERIMENTAL VERIFICATION OF THEORY

General

The values of D_x, D_y, and D_{xy} were determined experimentally for three corrugation patterns – the small vee, the large vee, and the square – shown in figure 3. A total of nine panels were tested. Each panel had a nominal depth of 1/2 inch. The small-vee corrugation had a nominal pitch of 1/2 inch; the large-vee and the square corrugations each had a nominal pitch of 1 inch. The variation in depth and pitch for a specimen did not exceed ±4 percent except for the edge corrugations. Some of the panels were fabricated of AISI type 347 stainless steel; others were fabricated of Inconel X. Spot welds of approximately 0.2-inch spacing were used to join the corrugated plate to the cover plate. Both the small-vee and the large-vee corrugations had single weld lines; the square corrugation had a double weld line as indicated in figure 3. The materials and average dimensions of all the test panels are given in table I. (The values of E and μ for type 347 stainless steel were obtained from ref. 4. The values of E, G, and μ for Inconel X were obtained from ref. 5.)

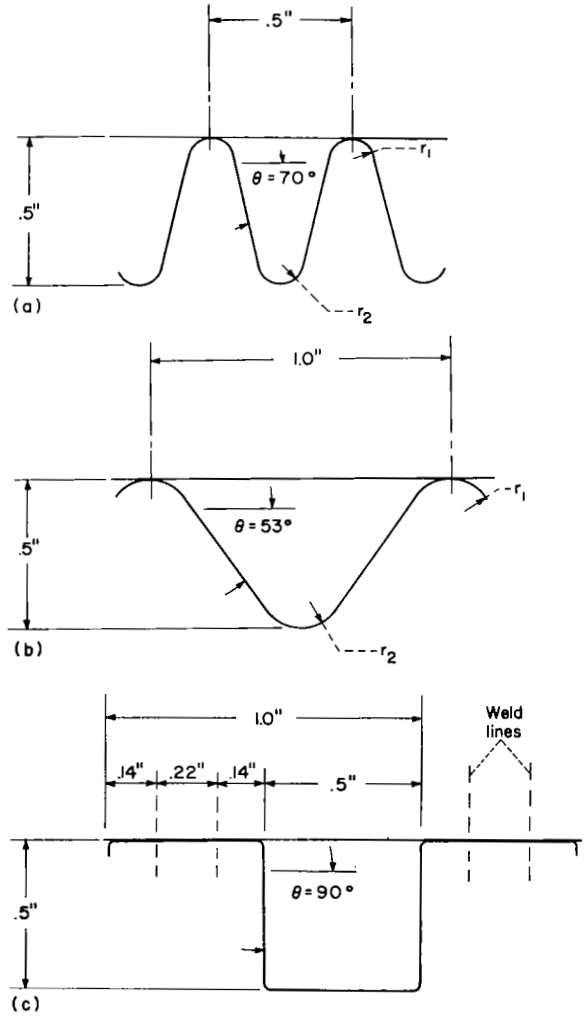

(a) Small vee; $r_1 = r_2 = 0.05"$.

(b) Large vee; $r_1 = r_2 = 0.14"$.

(c) Square; $r_1 = r_2 = 0"$.

Figure 3.- Corrugation shapes.

In order to assess the importance of Poisson's ratio in the determination of the measured bending stiffness, Poisson's ratios μ_x and μ_y were calculated for the test panels by using equations (17) and (20). These values are tabulated in table II. Note that the product $\mu_x\mu_y$ is less than 3×10^{-5} for all the test panels. Since small values of this product are typical of corrugation-stiffened panels, elementary beam theory can be used in the calculation of stiffnesses from measured deformations of the panel.

TABLE I.- AVERAGE DIMENSIONS OF EACH TEST PANEL

Test panel	Corrugation pattern	p, in.	a, in.	i, in.	g, in.	k, in.	d, in.	r_1, in.	r_2, in.	θ, deg	t_p, in.	t_c, in.	$\bar{y}$, in.
AISI type 347 stainless steel: E = 28.6 × 10^6; μ = 0.30													
D_x	Small vee	0.5290	0	0	0	0.4512	0.4900	0.0543	0.0543	68.79	0.0150	0.0150	0.1862
	Large vee	1.000	0	0	0	.4598	.4700	.1380	.1380	52.18	.0150	.0150	.1543
	Square	1.000	.1120	.1390	.2490	.4830	.4830	0	0	90.00	.0150	.0150	.1772
Inconel X: E = 31.0 × 10^6; G = 11.0 × 10^6; μ = 0.29													
D_y	Small vee	0.5000	0	0	0	0.4601	0.5040	0.0520	0.0520	70.73	0.01064	0.01064	0.1900
	Large vee	1.000	0	0	0	.4474	.4750	.1450	.1450	53.26	.01068	.01065	.1514
	Square	.9930	.1150	.1330	.2488	.5063	.5063	0	0	90.0	.01067	.01054	.1812
D_{xy}	Small vee	0.5020	0	0	0	0.4555	0.4981	0.0520	0.0520	70.37	0.0106	0.0106	0.1869
	Large vee	1.006	0	0	0	.4507	.4750	.1450	.1450	52.95	.0106	.0106	.1513
	Square	.9960	.1060	.1375	.2545	.4960	.4960	0	0	90.00	.0106	.0106	.1795

TABLE II.- CALCULATED VALUES OF POISSON'S RATIOS FOR EACH TEST PANEL

Test panel	Corrugation pattern	μ_x	μ_y	$\mu_x\mu_y$
D_x	Small vee	0.141	7.70 × 10^{-5}	1.08 × 10^{-5}
	Large vee	.156	15.2	2.38
	Square	.175	8.41	1.47
D_y	Small vee	0.130	3.16 × 10^{-5}	0.413 × 10^{-5}
	Large vee	.147	7.00	1.02
	Square	.169	3.65	.616
D_{xy}	Small vee	0.131	3.30 × 10^{-5}	0.434 × 10^{-5}
	Large vee	.147	7.04	1.04
	Square	.168	3.77	.632

Experimental Verification of Formula for D_x

Specimens.- The three specimens — one with each of three corrugation patterns — used for the evaluation of D_x were beams approximately 44 inches long and approximately 6 inches wide with corrugations parallel to the long dimension. Each specimen was fabricated of type 347 stainless-steel sheet which had an average thickness of 0.0150 inch with a variation in thickness of ±2 percent.

Test apparatus and procedure.- The test setup with pertinent dimensions is shown schematically in figure 4. A photograph of the apparatus with specimen is shown in figure 5. The beam was supported on two knife edges and loaded at the ends so as to obtain a region of pure bending moment between supports. The supports were 28.47 inches apart, and loads were applied with lead shot in increments of about 5 pounds to a maximum of about 60 pounds. Deflections of the beam were measured at the locations shown in figure 4 with dial gages having a sensitivity of 0.0001 inch. In order to take advantage of this high

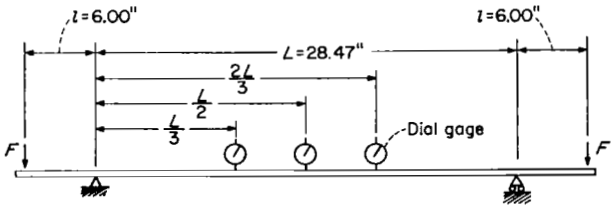

Figure 4.- Schematic diagram of test setup used for measuring D_x.

sensitivity, each dial gage was fitted with a screw with which the extension of the gage spindle could be adjusted until it just touched the surface of the beam. This positive screw action eliminates the effect of the internal friction of the dial gage and gives better repeatability of deflection measurements. Contact was detected by an electric circuit which

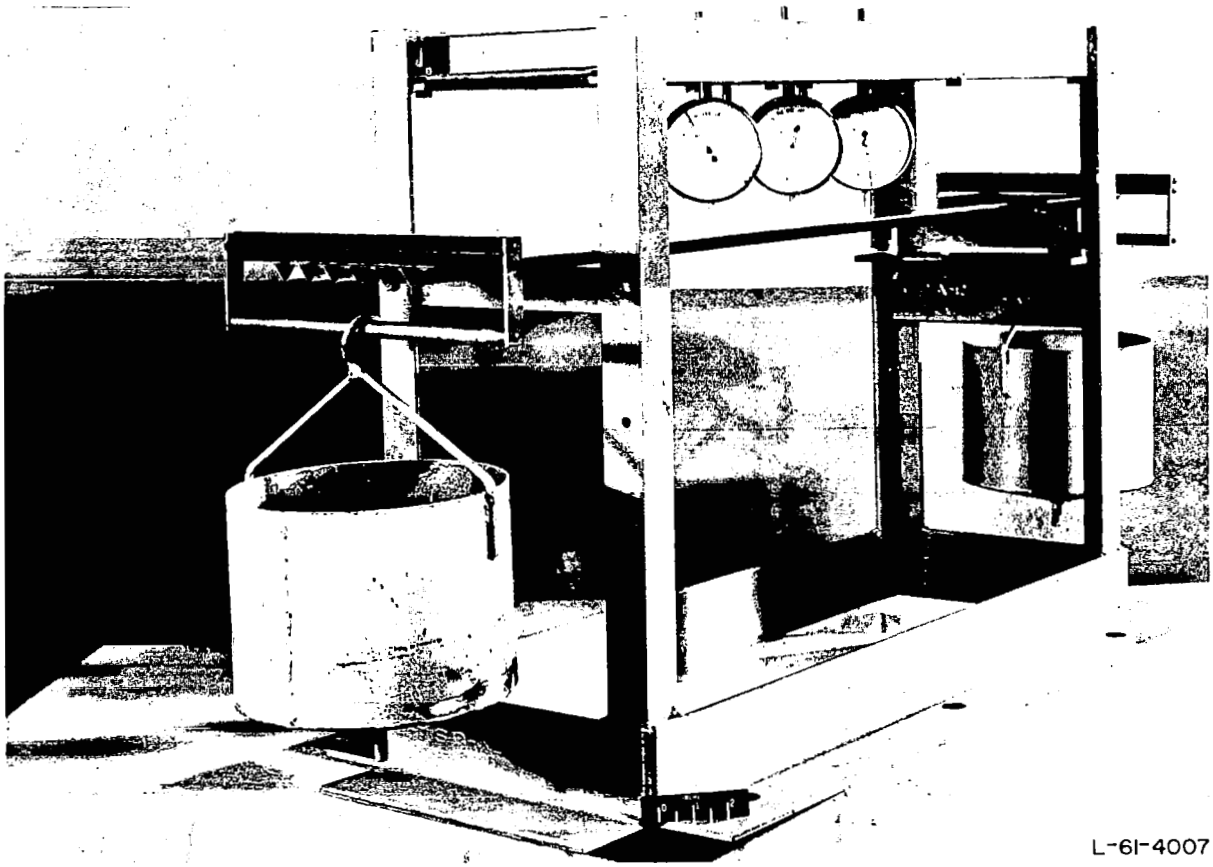

Figure 5.- Typical specimen and test setup used in the experimental determination of D_x.

activated an electron-ray tube. The electric detecting technique is similar to that described in reference 6.

The bending stiffness D_x was calculated from the following formula obtained from elementary beam theory for a uniform beam subjected to a constant moment:

$$D_x = \frac{(Fl)x_s(L - x_s)}{2cw_s} \tag{21}$$

where

F	load applied at each end of beam, lb
l	distance between load and support, in.
x_s	distance from left support to any station, in.
L	distance between supports, in.
w_s	deflection at station x_s, in.
c	width of beam, in.

Equation (21) was applied at three stations: $x_s = \frac{L}{3}, \frac{L}{2}$, and $\frac{2L}{3}$. The three values thus obtained differed from one another by less than 2 percent in any test; the average of the three values was taken as D_x. (This procedure is similar to that used in ref. 1.)

Discussion of results.- A comparison of the experimental and theoretical values of D_x for the three corrugation patterns are as follows:

For the small vee,

$$(D_x)_{exp} = 42{,}220 \pm 200 \text{ in-lb}$$

$$(D_x)_{th} = 42{,}230 \text{ in-lb}$$

For the large vee,

$$(D_x)_{exp} = 30{,}170 \pm 120 \text{ in-lb}$$

$$(D_x)_{th} = 30{,}280 \text{ in-lb}$$

For the square,

$$(D_x)_{exp} = 52{,}850 \pm 490 \text{ in-lb}$$

$$(D_x)_{th} = 51{,}730 \text{ in-lb}$$

As might be expected, the results of the tests for D_x compare very favorably with the theoretical values. The theoretical value of D_x fell within the range of experimental values for both the small-vee and the large-vee corrugation patterns. The theoretical value of D_x for the square corrugation pattern fell outside the experimental range by less than 2 percent (being slightly lower than the lowest experimental value).

Experimental Verification of Formula for D_y

Specimens.- The three panels used to determine the experimental values of D_y were 32 inches long and 6 inches wide. In this case the corrugations were normal to the long dimension of each panel. Each specimen was fabricated of Inconel X sheet which had an average thickness of about 0.0106 inch and a variation in thickness of ±3 percent. These test specimens are shown in figure 6.

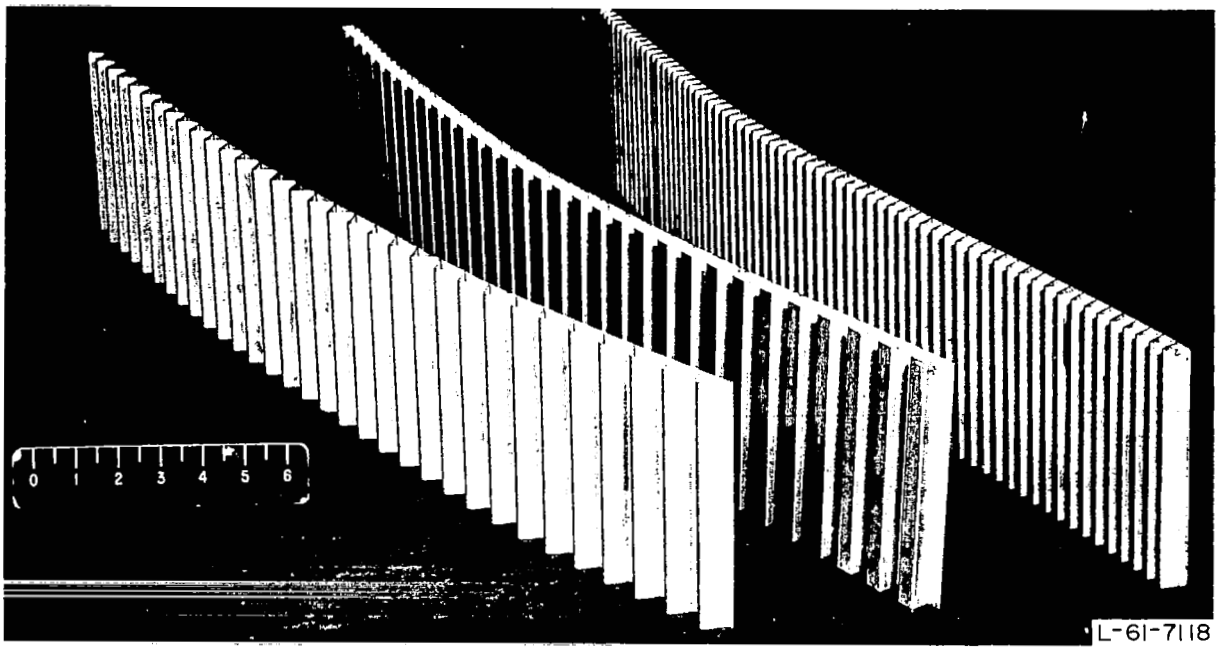

Figure 6.- Three specimens used in vibration tests for measuring D_y.

Test apparatus and procedure.- Vibration tests were performed on three panels in order to determine the experimental values of D_y. Each panel was hung by 8-foot-long nylon cords attached at the first-mode nodal points located 22 percent of the panel length from each end. This arrangement approximated free-free boundary conditions and is shown schematically in figure 7. The panels were vibrated with an air shaker (ref. 7), a noncontacting inductance pickup was used to detect the deflections, and a recording oscillograph with a paper speed of 7.5 inches per second was used to obtain frequencies and maximum amplitudes.

For each panel, several natural frequencies were obtained from which values of D_y could be calculated with the use of the following equation:

$$D_y = \frac{\rho}{c}\left(\frac{\omega_n}{\beta_n^2}\right)^2 \qquad (22)$$

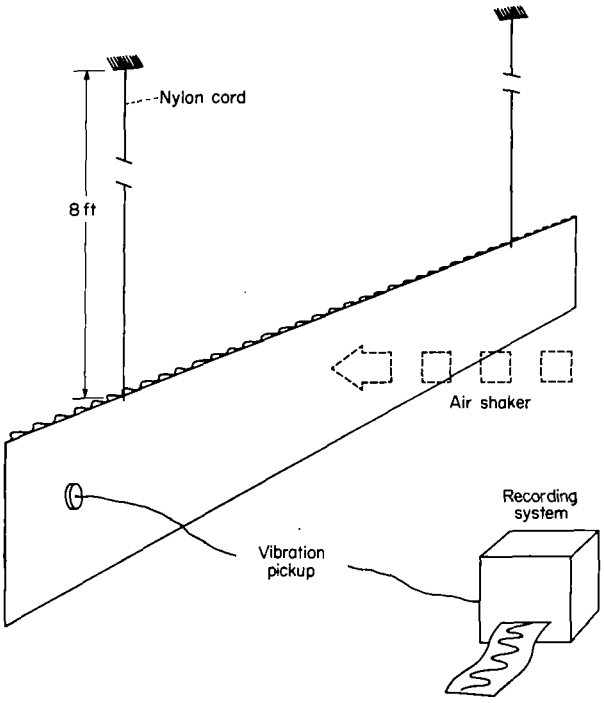

Figure 7.- Test setup used for measuring D_y.

where

ρ mass per unit length of panel, $lb\text{-}sec^2/in.^2$

ω_n natural frequency of nth mode of vibration of a panel, radians/sec

β_n a characteristic number from beam-vibration analysis (numerical values of β_n were obtained from ref. 8)

c width of panel, in.

Equation (22) is the frequency equation for beam vibration in which the beam stiffness has been replaced by the quantity cD_y.

Discussion of results.- Comparisons of the experimental and theoretical values of D_y for the three corrugation patterns are as follows:

For the small vee,

$$(D_y)_{exp} = 8.73 \text{ to } 9.36 \text{ in-lb}$$

$$(D_y)_{th} = 8.53 \text{ in-lb}$$

For the large vee,

$$(D_y)_{exp} = 11.12 \text{ to } 11.69 \text{ in-lb}$$

$$(D_y)_{th} = 11.26 \text{ in-lb}$$

For the square,

$$(D_y)_{exp} = 9.89 \text{ to } 10.83 \text{ in-lb}$$

$$(D_y)_{th} = 9.39 \text{ in-lb}$$

The experimental and theoretical values of D_y are also shown in figure 8.

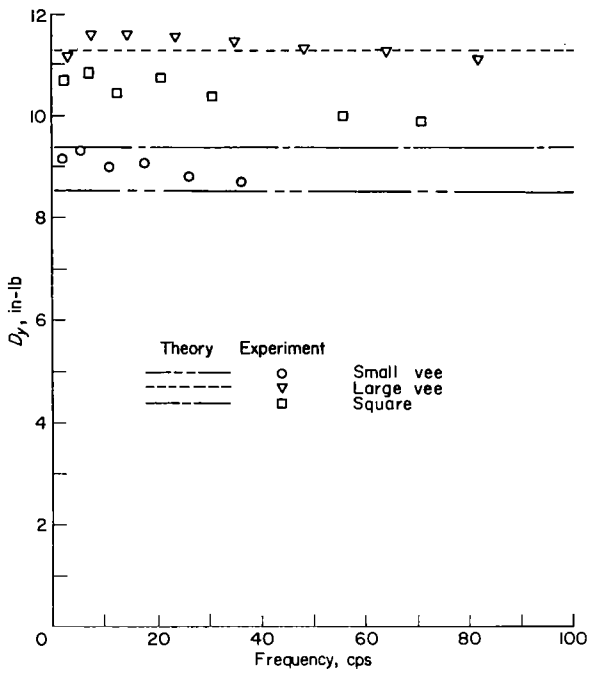

Figure 8.- Experimental and theoretical values of D_y.

As shown in this figure, the experimental values of D_y for a particular panel varied with frequency. However, each of the values of D_y was repeatable within $1\frac{1}{2}$ percent. Over most of the frequency range, the theoretical values of D_y are conservative, those for the square corrugation being the most conservative.

Experimental Verification of Formula for D_{xy}

Specimens.- Each specimen used for the evaluation of D_{xy} was fabricated of Inconel X sheet which had an average thickness of about 0.0106 inch with a variation in thickness of ± 3 percent. As in the tests for D_x and D_y, the three specimens tested represented the small-vee, the large-vee, and the square corrugation patterns. The panels were about 18 inches square.

As was pointed out in reference 3, when testing sandwich panels to determine torsional stiffness, the deformation must be restricted to pure twist. This restriction means that the panel must deform in such a way that normals to the middle plane remain normal; that is, no transverse shear deformation can be allowed. This same requirement applies to corrugation-stiffened panels, and it implies the need for two restrictions on the edges of the panel:

(1) The edges must remain straight.

(2) Each element of the edge cross section in the xz- or yz-plane must rotate through the same angle (the angle of twist of the panel).

For restriction (1), the two edges parallel to the x-axis are kept straight during testing by the corrugations running parallel to the x-axis. In order to keep the other two edges straight, it was necessary to attach aluminum plates along the edges of the panel parallel to the y-axis. These edge plates were sufficiently thin so that their torsional stiffness was negligible in comparison with that of the panel. The edge plates were attached to the panels with screws cast into plastic extending into the ends of the corrugation cells about 3/4 inch. The screws were inserted through holes in the edge plates, and nuts were mounted on the screws to allow the plates to be tightened against the corrugation cells. The tightness of these nuts in some cases plays a significant role in the achievement of restriction (2), and this role is discussed in detail in a subsequent

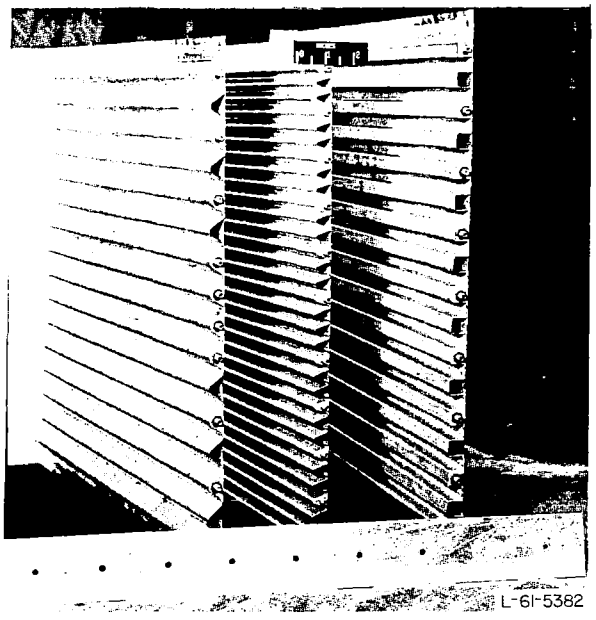

Figure 9.- Specimens (including edge plates) used to measure D_{xy}.

section entitled "Discussion of Results." The three panels with screws cast in the corrugations and aluminum edge plates are shown in figure 9.

Test apparatus and procedure.- The panels were supported at diagonally opposite corners, and an aluminum rod was suspended from the other two corners. Loads were applied by adding lead shot to a bucket hanging from the center of the aluminum rod.

Nine dial gages having a sensitivity of 0.0001 inch were used to measure the twist of the panel. The electrical system of measuring deflections noted in the section entitled "Experimental Verification of Formula for D_x" could not be used here because of the instability of the panel on its supports. When the electrical technique was used, small disturbances, such as dial gage contact and vibrations, caused the panel to rotate slightly about the line connecting the two supports during individual dial-gage readings. However, when all the dial gages made contact with the panel at the same time, the panel was stabilized and did not rotate while the dial gages were being read. The forces applied by dial-gage contact were nevertheless negligible. Figure 10 shows a typical specimen and test setup used in the torsion tests.

Loads were applied in 5-pound increments up to a maximum of 25 pounds. Deflections of the panel were measured at the nine points shown in figure 11. From the measured deflections, which were linear across the panel in the x- and y-directions, the angle of twist per unit length $\frac{\partial^2 w}{\partial x\, \partial y}$ was computed. The twisting stiffness was then obtained from the formula

$$D_{xy} = \frac{M_{xy}}{\partial^2 w / \partial x\, \partial y} \tag{23}$$

where the twisting moment M_{xy} is equal to one-half of the torque divided by the width of the cross section resisting the torque, or, equivalently, M_{xy} is equal to one-half of the load acting at each corner. (See ref. 3.)

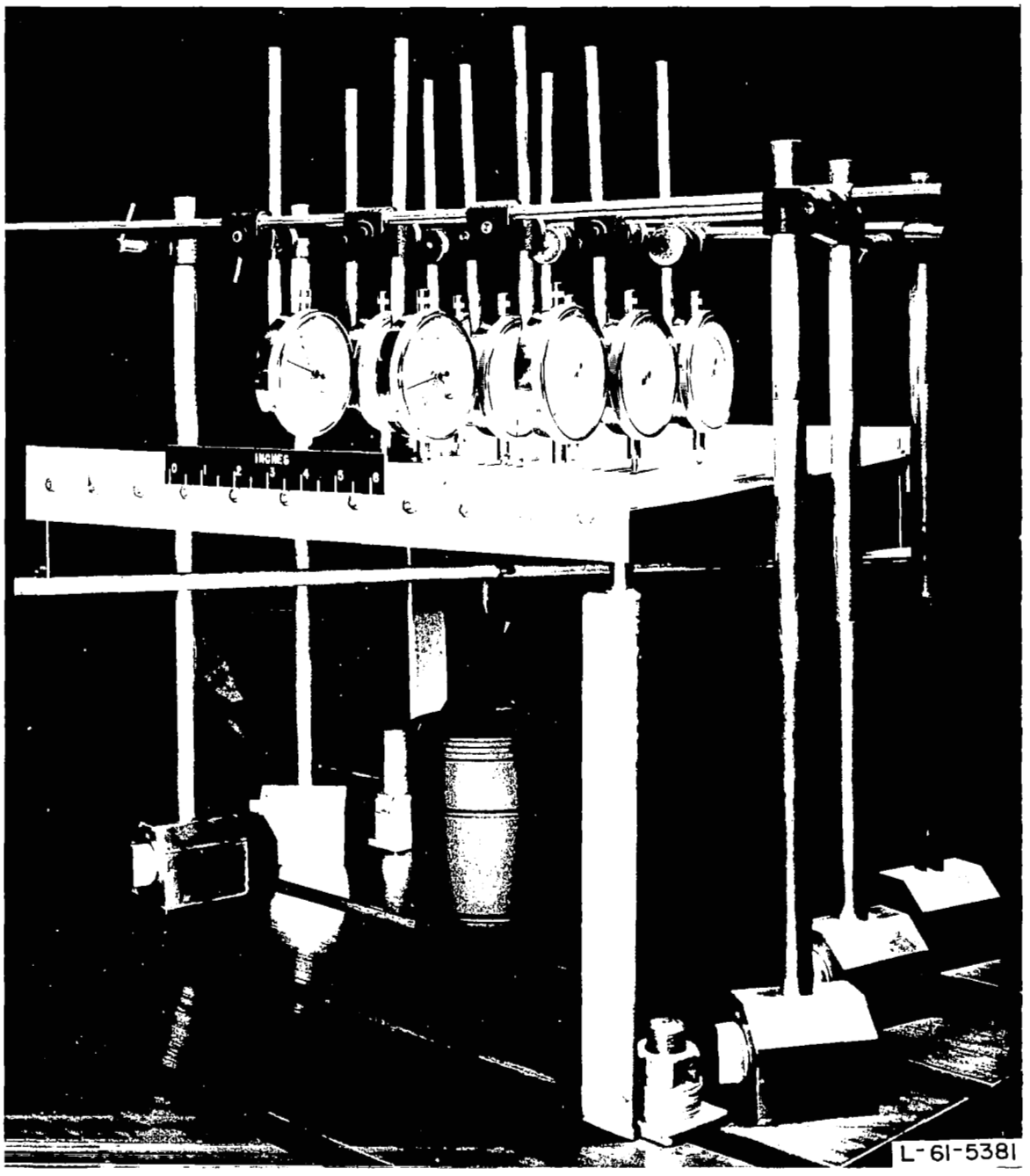

Figure 10.- Typical specimen and test setup used for measuring D_{xy}.

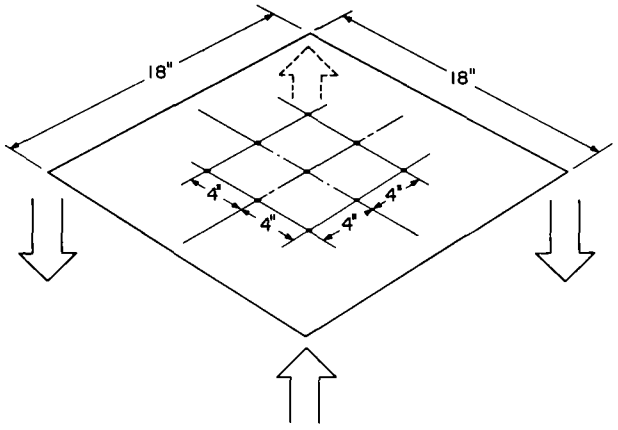

Figure 11.- Location of dial gages on torsion specimens.

Discussion of results.- Comparisons of the experimental and theoretical values of D_{xy} are as follows:

For the small vee,

$$(D_{xy})_{exp} = 5,125 \pm 50 \text{ in-lb}$$

$$(D_{xy})_{th} = 4,749 \text{ in-lb}$$

For the large vee,

$$(D_{xy})_{exp} = 5,837 \pm 13 \text{ in-lb}$$

$$(D_{xy})_{th} = 5,934 \text{ in-lb}$$

For the square,

$$(D_{xy})_{exp} = 5,750 \text{ in-lb}$$

$$(D_{xy})_{th} = 6,244 \text{ in-lb}$$

For the small-vee corrugation pattern the theoretical result is conservative by 7 percent, and for the large-vee pattern the difference between theory and experiment is less than 2 percent.

A more thorough discussion is required in order to understand the results of the tests on the square corrugation pattern. The stiffness measurements on the vee-shaped corrugations were essentially independent of whether the nuts on the edge-plate mountings were tight or loose. For the square corrugation pattern, on the other hand, large variations in the apparent torsional stiffness[1] were measured and depended on the tightness of the nuts. For instance, in tests in which the edge-plate connections were loose, values of the apparent torsional stiffness as low as 2,900 in-lb were obtained on the square corrugation specimen. The experimental value reported above, 5,750 in-lb, was obtained from a specimen having tight edge-plate connections and having screws cast in every cell, rather than in every other cell as shown in figure 9.

The square pattern falls into a category of shapes for which special precautions must be taken to comply with restriction (2) discussed under "Specimens." The flat portion between the corrugation cells appears to be significant in this

[1]Since D_{xy} is a stiffness associated with a deformation which conforms to restrictions (1) and (2) stated in the section entitled "Specimens," a measured stiffness based on overall deformations which do not conform to the restrictions is referred to as the "apparent" value of D_{xy}.

regard. Under torsional loads the deformation of the flat portion may be partially independent of the deformation of the cells. The panel as a whole, therefore, may have a larger angle of twist than the individual cells. This situation is illustrated in sketch 1 of a typical cross section of a panel having a flat portion between cells. The dashed outline denotes the undeformed shape and the solid outline denotes an exaggerated deformed shape emphasizing the possible difference in behavior between the flat portions and the cells. With the dialgage techniques used in this investigation, it is likely that angle ① is measured although the cells rotate only through the smaller angle ②.

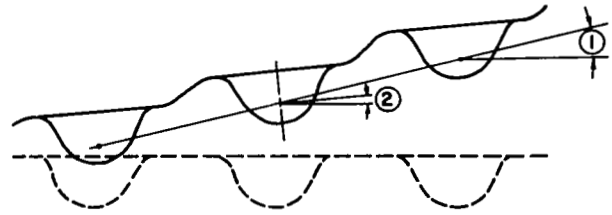

Sketch 1.

The edge plates provided a reasonably effective means for eliminating the independent action just discussed. The connections between the panel and edge plates were such that nuts could be used to tighten the edge plates against the corrugation cells. When the connections were tight, rotation of the edge plates forced the cells having connections to rotate also, but, because of unavoidable slippage, not necessarily through the same angle as the edge plates. This slippage, even when the connections were tight, may account for the fact that the experimental value of D_{xy} for the square corrugation specimen was 9 percent lower than the theoretical value.

Since the stiffness measurements on the panels with the vee-shaped corrugations were not affected by the degree of tightness of the edge plates, it appeared that additional experimental information on the influence of flat portions between the cells could be obtained by testing a panel consisting of alternating vee-shaped corrugations and flat portions. Consequently, a panel was tested which had a cross-section configuration as indicated in sketch 2. The external dimensions of this panel were similar to those of the other panels used in the torsion tests. The result of this test was that the apparent torsional stiffness with connections loose was about three-fourths of the apparent torsional stiffness with connections tight. This result substantiates the idea that the partially independent action of the flat portions and the cells is an important factor in the torsional behavior of corrugation-stiffened panels which have a flat portion between corrugation cells.

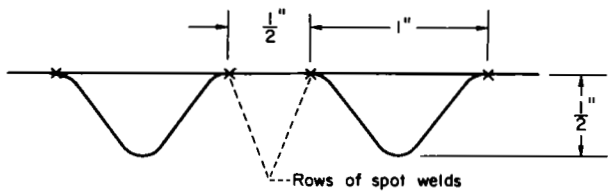

Sketch 2.

CONCLUDING REMARKS

This report presents theoretical formulas for five orthotropic elastic constants associated with pure bending and pure twist for a corrugation-stiffened panel. The constants are the bending stiffnesses parallel to and normal to the corrugation direction $(D_x$ and $D_y)$, the twisting stiffness (D_{xy}), and the Poisson's ratios associated with bending $(\mu_x$ and $\mu_y)$. Theoretical values of D_x, D_y, and D_{xy} are compared with experimental results for three corrugation patterns – two vee shapes and a square shape – and generally showed good agreement. It is shown that for corrugation-stiffened panels typical of practical construction, the product $\mu_x\mu_y$ is very small compared with unity.

Langley Research Center,
National Aeronautics and Space Administration,
Langley Station, Hampton, Va., November 21, 1962.

APPENDIX A

DERIVATION OF FORMULA FOR D_x

The panel bending stiffness D_x is simply the bending stiffness per unit width of a beam having the cross-sectional shape shown in figure 2. When the panel is considered to be made up of a series of cells and the contributions of each element of the cross section are totaled, the following equation is obtained:

$$D_x = \frac{2E_p}{p}\left[\frac{(a+b)t_p^3}{12} + \left(\bar{y} - \frac{t_p}{2}\right)^2 (a+b)t_p\right] + \frac{2E_c}{p}\left[\frac{(a+i)t_c^3}{12} + \left(e_1 + r_1\right)^2 (a+i)t_c\right.$$

$$+ t_c r_1^3\left(\frac{\theta}{2} + \frac{\sin 2\theta}{4}\right) + 2t_c e_1 r_1^2 \sin\theta + e_1^2 r_1 \theta t_c + \frac{t_c}{12} k^3 \sin^2\theta + \frac{kt_c^3}{12}\cos^2\theta$$

$$+ \left(t_p + \frac{t_c}{2} + j + \frac{k}{2}\sin\theta - \bar{y}\right)^2 kt_c + t_c r_2^3\left(\frac{\theta}{2} + \frac{\sin 2\theta}{4}\right) + 2t_c e_2 r_2^2 \sin\theta$$

$$\left. + e_2^2 r_2 \theta t_c + \frac{gt_c^3}{12} + \left(e_2 + r_2\right)^2 t_c g\right] \tag{A1}$$

where

$$\bar{y} = \frac{\left[\begin{array}{l} \frac{E_p}{E_c}\frac{t_p^2}{2}(b+a) + \left(t_p + \frac{t_c}{2}\right)(a+i)t_c + \left(t_p + \frac{t_c}{2} + r_1 - \frac{r_1 \sin\theta}{\theta}\right) r_1 \theta t_c \\ + \left(t_p + \frac{t_c}{2} + j + \frac{n-j}{2}\right) kt_c + \left(t_p + \frac{t_c}{2} + d - r_2 + \frac{r_2 \sin\theta}{\theta}\right) r_2 \theta t_c + \left(t_p + \frac{t_c}{2} + d\right) gt_c \end{array}\right]}{\frac{E_p}{E_c} t_p(b+a) + (a+i)t_c + r_1\theta t_c + kt_c + r_2\theta t_c + gt_c} \tag{A2}$$

APPENDIX B

DERIVATION OF FORMULA FOR D_y

A single cell of a corrugation-stiffened panel under pure bending is shown in figure 12(a). As indicated, each cell must carry the total bending moment M_y applied to the panel. In this derivation, the term "plate" refers to the flat cover plate to which the corrugation is attached and the term "panel" refers to the composite structure. At the weld line, where the plate is joined to the corrugation, the moment is distributed to the corrugation and to the plate in proportion to their respective stiffnesses. The plate and the corrugation are now treated as separate structures each having its own force system and deformation as shown in figure 12(b). The curvature in the x-direction resulting from M_y is considered to be zero. The forces and deformations are related in the following way:

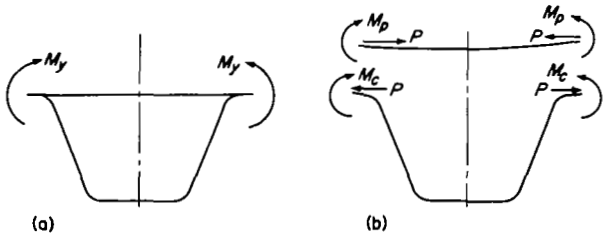

(a) Undeformed composite cell with M_y loading.

(b) Loads and deformations of cell components.

Figure 12.- Loading on corrugation cell.

(1) The slopes of the plate and corrugation are equal at the weld line.

(2) The extensions of the plate and corrugation are equal at the weld line.

(3) The moment carried by the corrugation plus the moment carried by the plate equals the moment carried by the panel; that is,

$$M_c + M_p = M_y \tag{B1}$$

(4) The slope at the weld line for each element is the same as the slope of the panel which is determined by D_y and M_y.

(5) Equal and opposite (in-plane) loads P act at the weld line. Symmetry and overall equilibrium of the plate or corrugation normal to the panel dictate that no normal forces act at the weld line.

The corrugation is analyzed first. The bending strain energy U caused by the loads P and moments M_c is computed. The slopes and extensions caused by bending are then obtained by taking the appropriate partial derivatives of the strain energy. The strain energy is calculated from

$$U = \frac{1}{2D_c} \int (\text{Moment})^2 ds \tag{B2}$$

where D_c is the plate bending stiffness of the corrugation material, and the integration is taken over the corrugation cross section. In equation (B2),

D_c rather than $(EI)_c$ is used because the bending is considered to be cylindrical, that is, $\frac{\partial^2 w}{\partial x^2} = 0$. If the corrugation is divided into elements AB, BC, CD, DE, and EF, as shown in figure 13, the contribution of each corrugation element to the strain energy is given by the following equations for the case in which the panel has only a single weld ($a = 0$):

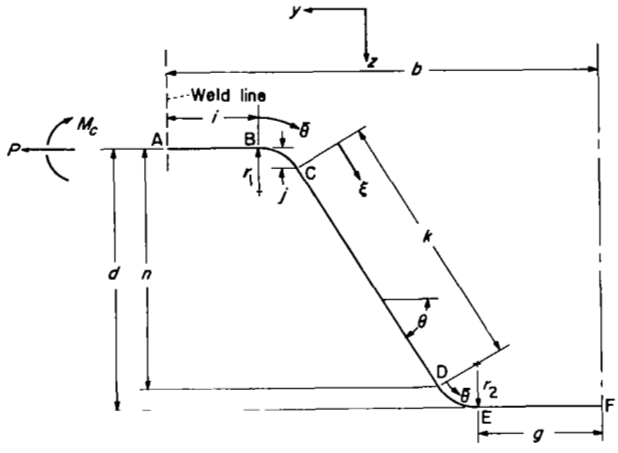

Figure 13.- One-half of a single-weld-line-type corrugation cell (appendix B).

For element AB,

$$U = \frac{1}{2D_c} \int_0^i M_c^2 dy \qquad (B3)$$

For element BC,

$$U = \frac{1}{2D_c} \int_0^\theta \left[M_c - Pr_1(1 - \cos \bar{\theta})\right]^2 r_1 \, d\bar{\theta} \qquad (B4)$$

For element CD,

$$U = \frac{1}{2D_c} \int_0^k \left[M_c - P(j + \xi \sin \theta)\right]^2 d\xi \qquad (B5)$$

For element DE,

$$U = \frac{1}{2D_c} \int_0^\theta \left(M_c - P\left\{n + r_2\left[\cos(\theta - \bar{\theta}) - \cos \theta\right]\right\}\right)^2 r_2 \, d\bar{\theta} \qquad (B6)$$

For element EF,

$$U = \frac{1}{2D_c} \int_0^g \left(M_c - P\,d\right)^2 dy \qquad (B7)$$

Expanding, integrating, and totaling these contributions gives

$$U = \frac{1}{2D_c}\left\{M_c^2 i + r_1 M_c^2 \theta - 2M_c P r_1^2(\theta - \sin\theta) + P^2 r_1^3\left(\frac{3\theta}{2} - 2\sin\theta + \frac{\sin 2\theta}{4}\right)\right.$$

$$+ M_c^2 k - 2PM_c\left(jk + \frac{k^2}{2}\sin\theta\right) + P^2\left(j^2 k + jk^2 \sin\theta + \frac{k^3}{3}\sin^2\theta\right) + r_2 M_c^2 \theta$$

$$- 2r_2 M_c P\left(n\theta - r_2\theta\cos\theta + r_2\sin\theta\right) + r_2 P^2\left[n^2\theta - 2nr_2\theta\cos\theta + 2nr_2\sin\theta\right.$$

$$\left.\left. + \frac{r_2^2}{2}\left(3\theta - 3\sin\theta\cos\theta - 2\theta\sin^2\theta\right)\right] + M_c^2 g - 2M_c P g d + P^2 g d^2\right\} \qquad (B8)$$

According to Castigliano's theorem, the slope of the corrugation at the weld line is given by $-\frac{\partial U}{\partial M_c}$ where the sign is determined from the coordinate system shown in figure 13. The slope of the plate at the weld line is given by $-\frac{M_p b}{D_p}$ and, because of the weld, is equal to the slope of the corrugation at the weld line. Thus,

$$\frac{M_p b}{D_p} = \frac{\partial U}{\partial M_c}$$

$$= \frac{1}{D_c}\left[M_c i + r_1 M_c \theta - P r_1^2(\theta - \sin\theta) + M_c k - P\left(jk + \frac{k^2}{2}\sin\theta\right)\right.$$

$$\left. + r_2 M_c \theta - r_2 P\left(n\theta - r_2\theta\cos\theta + r_2\sin\theta\right) + M_c g - P g d\right] \qquad (B9)$$

Another equation can be obtained by equating the extensions of the corrugation and plate at the weld line. In this analysis, only the corrugation extension caused by bending is considered and the plate extension is neglected. This assumption seems justified because extensions caused by direct strains in the plate are of the same order of magnitude as the extensions caused by direct strains in the elements of the corrugation. The direct strains in the corrugation elements are negligible compared with the bending deformations. However, when the depth d of the corrugation is small, the extensions caused by direct strains have to be considered.

The extension of the corrugation at the weld line is given by $\frac{\partial U}{\partial P}$. Equating the extensions of the corrugation and plate at the weld line gives

$$\frac{\partial U}{\partial P} = \frac{1}{D_c}\left\{-r_1^2 M_c(\theta - \sin\theta) + Pr_1^3\left(\frac{3\theta}{2} - 2\sin\theta + \frac{\sin 2\theta}{4}\right) - M_c\left(jk + \frac{k^2}{2}\sin\theta\right)\right.$$

$$+ P\left(j^2k + jk^2\sin\theta + \frac{k^3}{3}\sin^2\theta\right) - r_2M_c\left(n\theta - r_2\theta\cos\theta + r_2\sin\theta\right)$$

$$+ r_2P\left[n^2\theta - 2nr_2\theta\cos\theta + 2nr_2\sin\theta + \frac{r_2^2}{2}\left(3\theta - 3\sin\theta\cos\theta - 2\theta\sin^2\theta\right)\right]$$

$$\left. - M_cgd + Pgd^2\right\}$$

$$= 0 \qquad \text{(B10)}$$

Grouping the coefficients of P and M_c yields

$$P = HM_c \qquad \text{(B11)}$$

where

$$H = \frac{r_1^2(\theta - \sin\theta) + jk + \frac{k^2}{2}\sin\theta + r_2\left(n\theta - r_2\theta\cos\theta + r_2\sin\theta\right) + gd}{\left[r_1^3\left(\frac{3\theta}{2} - 2\sin\theta + \frac{\sin 2\theta}{4}\right) + j^2k + jk^2\sin\theta + \frac{k^3}{3}\sin^2\theta + r_2n^2\theta\right.}$$

$$\left. - 2nr_2^2\theta\cos\theta + 2nr_2^2\sin\theta + \frac{r_2^3}{2}\left(3\theta - 3\sin\theta\cos\theta - 2\theta\sin^2\theta\right) + gd^2\right] \qquad \text{(B12)}$$

Substituting HM_c for P in equation (B9) gives

$$M_p = \frac{M_c}{b}\frac{D_p}{D_c}X \qquad \text{(B13)}$$

where

$$X = i + \theta\left(r_1 + r_2\right) + k + g - H\left[r_1^2(\theta - \sin\theta) + jk\right.$$

$$\left. + \frac{k^2}{2}\sin\theta + r_2\left(n\theta - r_2\theta\cos\theta + r_2\sin\theta\right) + gd\right] \qquad \text{(B14)}$$

If the expression given in equation (B13) is substituted for M_p in the equation

$$M_c + M_p = M_y$$

the result is

$$M_c\left(1 + \frac{D_p}{bD_c} X\right) = M_y \tag{B15}$$

Because the curvature in the x-direction is considered to be zero, the moment-curvature relationship for the panel is

$$M_y = -\frac{D_y}{1 - \mu_x\mu_y} \frac{\partial^2 w}{\partial y^2} \tag{B16}$$

By considering $\frac{\partial^2 w}{\partial y^2}$ to be constant and by substituting the expression for M_y given by equation (B15) into equation (B16), the slope of the panel at the weld line is given by

$$\left.\frac{\partial w}{\partial y}\right|_{y=b} = -M_c\left(1 + \frac{D_p}{bD_c} X\right)\frac{b}{D_y'}\left(1 - \mu_x\mu_y\right) \tag{B17}$$

Equating the slopes of the corrugation and panel at the weld line gives

$$\frac{M_c}{D_c} X = M_c\left(1 + \frac{D_p}{bD_c} X\right)\frac{b}{D_y'}\left(1 - \mu_x\mu_y\right) \tag{B18}$$

where D_y' is the bending stiffness per unit width of the panel if the dimension a equals zero, that is for the case in which the panel has a single weld line instead of a double weld line. Equation (B18) can be solved for $\frac{D_y'}{1 - \mu_x\mu_y}$ to give

$$\frac{D_y'}{1 - \mu_x\mu_y} = \frac{bD_c}{X} + D_p \tag{B19}$$

For the case in which the panel has a double weld line, the dimension a does not equal zero, and the segment of length $2a$ has to be considered. This segment is treated as a composite beam. The location of the neutral axis for such a beam is as follows (see ref. 9):

$$\bar{z} = \frac{\frac{t_p^2}{2} + \frac{E_c}{E_p}\left(t_p + \frac{t_c}{2}\right)t_c}{t_p + \frac{E_c}{E_p}t_c} \tag{B20}$$

where $\bar{z}$ is the distance from the outer surface of the plate to the neutral axis as shown in sketch 3.

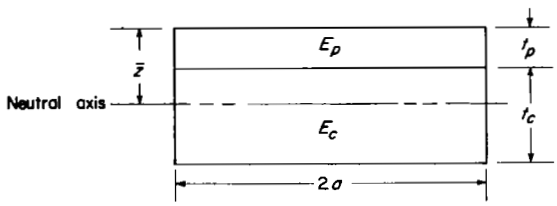

Sketch 3.

The bending strain ϵ_y at a distance z from the neutral axis is given by

$$\epsilon_y = \frac{z}{r_y} \tag{B21}$$

where r_y is the radius of curvature in the y-direction.

Again, when bending is considered to be cylindrical, the bending strain ϵ_x equals zero. Therefore, with the use of Hooke's law and equation (B21), the bending stress in the y-direction is given by

$$\sigma_y = \frac{Ez}{(1 - \mu^2)r_y} \tag{B22}$$

The normal stresses distributed over the ends of the segment must produce couples equal to the applied moment, or

$$M_y = \int_{\bar{z}-t_p-t_c}^{\bar{z}-t_p} \sigma_c z \, dz + \int_{\bar{z}-t_p}^{\bar{z}} \sigma_p z \, dz \tag{B23}$$

where σ_c is the stress in the y-direction acting on the corrugation and σ_p is the stress in the y-direction acting on the plate.

Substituting equation (B22) into equation (B23) and using the appropriate values of E and μ gives

$$M_y = \left(\frac{E_c}{1 - \mu_c^2}\int_{\bar{z}-t_p-t_c}^{\bar{z}-t_p} z^2 dz + \frac{E_p}{1 - \mu_p^2}\int_{\bar{z}-t_p}^{\bar{z}} z^2 dz\right)\frac{1}{r_y} \tag{B24}$$

By comparing equation (B24) with the well-known moment-curvature relationship for cylindrical bending of isotropic plates, that is

$$M_y = \frac{D}{r_y} \tag{B25}$$

the bending stiffness of the segment between weld lines can be defined as

$$\frac{D_y''}{1 - \mu_x\mu_y} = \frac{E_c}{1 - \mu_c^2} \int_{\bar{z}-t_p-t_c}^{\bar{z}-t_p} z^2 dz + \frac{E_p}{1 - \mu_p^2} \int_{\bar{z}-t_p}^{\bar{z}} z^2 dz \tag{B26}$$

where D_y'' is the bending stiffness per unit width of a beam cut from the segment of length 2a. After performing the integration, $\frac{D_y''}{1 - \mu_x\mu_y}$ is given as

$$\frac{D_y''}{1 - \mu_x\mu_y} = \frac{E_c}{3\left(1 - \mu_c^2\right)}\left(t_c^3 + 3t_p t_c^2 + 3t_p^2 t_c + 3\bar{z}^2 t_c - 6\bar{z}t_p t_c - 3\bar{z}t_c^2\right)$$

$$+ \frac{E_p}{3\left(1 - \mu_p^2\right)}\left(t_p^3 - 3\bar{z}t_p^2 + 3\bar{z}^2 t_p\right) \tag{B27}$$

For the case in which the cover-plate material is the same as the corrugation material,

$$\frac{D_y''}{1 - \mu_x\mu_y} = \frac{E\left(t_c + t_p\right)^3}{12(1 - \mu^2)} \tag{B28}$$

The change in slope between the end and the center of the segment of length 2a is given by

$$\frac{M_y a\left(1 - \mu_x\mu_y\right)}{D_y''} \tag{B29}$$

The change in slope between the weld line and the center line of the corrugation cell is

$$\frac{M_y b\left(1 - \mu_x\mu_y\right)}{D_y'} \tag{B30}$$

The total change in slope between the center of the segment of length 2a and the center line of the corrugation cell is the sum of expressions (B29) and (B30):

$$M_y\left(\frac{a}{D_y''} + \frac{b}{D_y'}\right)\left(1 - \mu_x\mu_y\right) \tag{B31}$$

Dividing expression (B31) by one-half the pitch gives the change in slope per unit length. Since the change in slope per unit length is also equal to $\frac{M_y\left(1 - \mu_x\mu_y\right)}{D_y}$, there results

$$\frac{M_y}{D_y} = \frac{M_y}{a + b}\left(\frac{a}{D_y''} + \frac{b}{D_y'}\right) \tag{B32}$$

The bending stiffness D_y is then given by

$$D_y = \frac{a + b}{\frac{a}{D_y''} + \frac{b}{D_y'}} \tag{B33}$$

where D_y'' is given by equation (B27) or (B28) and D_y' is given by equation (B19). It is shown in appendix D that for a corrugation-stiffened panel, the product $\mu_x\mu_y$ is usually small compared with unity and can be neglected in the computation of D_y' and D_y''.

APPENDIX C

DERIVATION OF FORMULA FOR D_{xy}

It was mentioned in the body of this report that a corrugation-stiffened panel might be considered as a series of cells. Each of these cells has the torsional rigidity GJ of a thin-walled tube. The torsion-twist relationship for a thin-walled tube is given by

$$T = GJ\theta_l \tag{C1}$$

where

T total torque on a cell

GJ total torsional rigidity of a cell

θ_l angle of twist per unit length of a cell

The torsion-twist relationship can also be expressed as

$$\overline{T} = \overline{GJ}\theta_l \tag{C2}$$

where the bars indicate that the quantities T and GJ are divided by the width of the cross section considered.

The torsion-twist relationship for an orthotropic panel is

$$M_{xy} = D_{xy} \frac{\partial^2 w}{\partial x \, \partial y} \tag{C3}$$

The torque per unit width $\overline{T}$ is considered to act on only two edges of a rectangular orthotropic panel whereas, to be consistent with the differential equation for lateral deflections, the twisting moment M_{xy} is considered to act on all four edges. Therefore, for the same deformation to take place, the torque per unit width $\overline{T}$ must equal twice the twisting moment M_{xy}. A comparison of equations (C2) and (C3) then yields

$$D_{xy} = \frac{\overline{GJ}}{2} \tag{C4}$$

where

$$\overline{GJ} = \frac{4A^2}{p \oint \frac{ds}{Gt}} = \text{Torsion constant per unit width of cross section (from Bredt theory, see ref. 10)} \tag{C5}$$

in which

A area enclosed by corrugation cell (see sketch 4)

ds elemental length along center line of sheet making up corrugation cell

t thickness of sheet associated with ds

p pitch of corrugation pattern

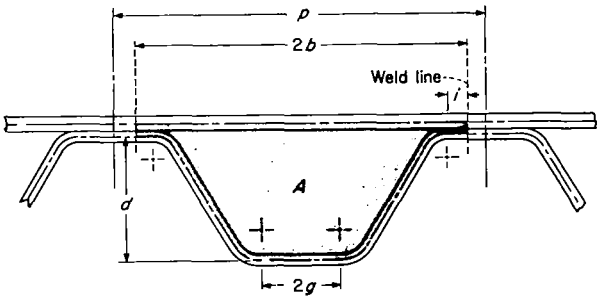

Sketch 4.

The integral is taken along the center line of the corrugation cell. The shear modulus G is retained inside the integral to account for the possibility of different materials for the plate and corrugation. The area A is given by

$$A = b\left(t_c + t_p\right) + d\left[b + g - i + \left(r_2 - r_1\right)\tan\frac{\theta}{2}\right] + 2\left(r_1^2 - r_2^2\right)\tan\frac{\theta}{2} + \left(r_2^2 - r_1^2\right)\theta \tag{C6}$$

The integral along the center line of the corrugation cell is given by

$$\oint \frac{ds}{Gt} = \frac{2b}{G_p t_p} + \frac{2}{G_c t_c}\left(i + r_1\theta + r_2\theta + k + g\right) \tag{C7}$$

Substituting equations (C5) to (C7) into equation (C4) gives

$$D_{xy} = \frac{\overline{GJ}}{2}$$

$$= \frac{\frac{G_p}{p}\left\{b\left(t_c + t_p\right) + d\left[b + g - i + \left(r_2 - r_1\right)\tan\frac{\theta}{2}\right] + 2\left(r_1^2 - r_2^2\right)\tan\frac{\theta}{2} + \left(r_2^2 - r_1^2\right)\theta\right\}^2}{\frac{b}{t_p} + \frac{G_p}{t_c G_c}\left(i + r_1\theta + r_2\theta + k + g\right)} \tag{C8}$$

APPENDIX D

DERIVATION OF FORMULAS FOR μ_x AND μ_y

For small deformations, μ_x may be defined as the ratio of the panel curvature in the y-direction to the panel curvature in the x-direction when the moment M_x is the only loading on the panel. The definition of μ_y is obtained by interchanging x and y in the definition of μ_x. Just as in the case of isotropic plates, these definitions of μ_x and μ_y are applicable only when the deformations are small.

An expression for μ_x is obtained by use of a method which has some similarities to that used in the derivation of D_y. Consider a rectangular corrugation-stiffened panel and assume the plane $x = 0$ passes through the center of the panel. (See fig. 1.) A moment M_x is assumed to be applied to the panel and yields a curvature K in the x-direction. The curvature in the yz-plane, which is independent of x, is calculated and this curvature divided by K is the Poisson's ratio μ_x. In order to calculate the curvature in the yz-plane due to M_x, the corrugation and plate which comprise the panel are first considered to be separated at the weld lines and to act independently. The axial-strain distribution caused by M_x is applied to the corrugation and plate, and their deformations are calculated at $x = 0$. It is found that redundant forces and moments are necessary to match up the extensions in the y-direction and the slopes in the yz-plane at the weld lines. These forces and moments are also determined by the use of Castigliano's theorem as was done in the derivation of D_y. The other bending Poisson's ratio μ_y can be determined from the relation $\frac{\mu_y}{D_y} = \frac{\mu_x}{D_x}$ which can be derived from the theorem of reciprocity. (See ref. 3.)

Deformation of Corrugation

A moment M_x acting on the corrugation, figure 14(a), is assumed to give a linear strain distribution ϵ_x as shown in figure 14(b). If the corrugation and plate are separated, moments M and loads P act at the weld line as shown in figure 14(c). The corrugation, which is considered to have a single weld line at present, is analyzed first. Figure 15 gives the dimensions of the corrugation cell and divides the cell into elements AB, BC, CD, DE, and EF. For all elements, the axial strain ϵ_x is considered to be uniform through the thickness t_c or t_p and equal to the axial strain of the middle surface of the element. The deformation of the corrugation caused by the axial strain ϵ_x is now considered.

Element AB.- The axial strain ϵ_x in element AB is given by

$$\epsilon_x = -K(e_1 + r_1) \tag{D1}$$

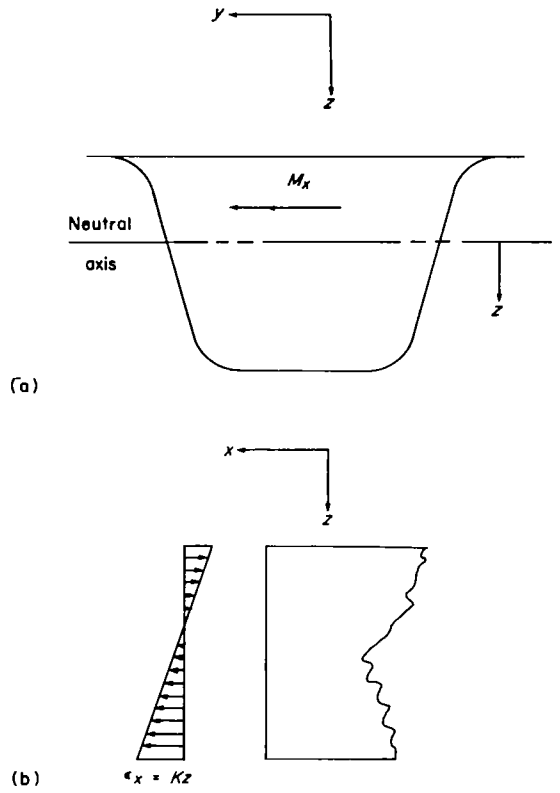

(a) Undeformed composite cell with M_x loading.

(b) Strain distribution resulting from M_x.

(c) Loading at weld line and deformations of cell components.

Figure 14.- Loading on corrugation cell.

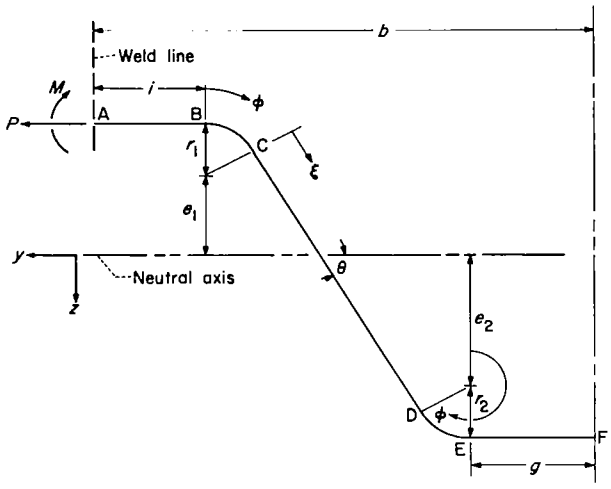

Figure 15.- One-half of a single-weld-line-type corrugation cell (appendix D).

where K is the primary curvature resulting from M_x. Considering σ_y to be zero and using the stress-strain relations for plane stress gives

$$\epsilon_y = K\mu_c\left(e_1 + r_1\right) \qquad (D2)$$

The extension of element AB in the y-direction is then given by

$$\delta_1 = Ki\mu_c\left(e_1 + r_1\right) \qquad (D3)$$

Element BC.- Element BC is analyzed as a sector of a cylinder deformed by a uniform axial load and a bending moment. Coordinates and displacements are shown in sketch 5.

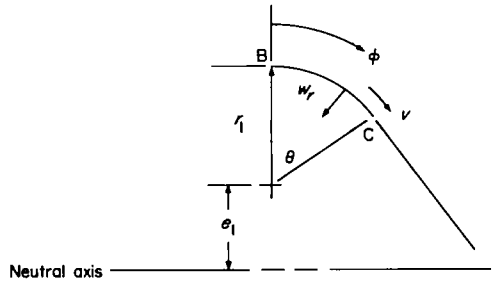

Sketch 5.

The strain-displacement relationships for element BC are

$$\epsilon_x = \frac{\partial u}{\partial x} \tag{D4}$$

$$\epsilon_\phi = \frac{1}{r_1}\frac{\partial v}{\partial \phi} - \frac{w_r}{r_1} \tag{D5}$$

$$\gamma_{x\phi} = \frac{1}{r_1}\frac{\partial u}{\partial \phi} + \frac{\partial v}{\partial x} \tag{D6}$$

The strain ϵ_x is given by

$$\epsilon_x = -K\left(e_1 + r_1 \cos \phi\right) \tag{D7}$$

Thus, from equation (D4)

$$u = -Kx\left(e_1 + r_1 \cos \phi\right) + f(\phi) \tag{D8}$$

At $x = 0$, $u = 0$; therefore, $f(\phi) = 0$.

With the assumption of $\gamma_{x\phi} = 0$, equations (D6) and (D8) give

$$v = v_1(\phi) - \frac{Kx^2}{2} \sin \phi \tag{D9}$$

where $v_1(\phi)$ is an arbitrary function of ϕ only. Since all strains are assumed to be functions of ϕ only, examination of equations (D5) and (D9) leads to the conclusion that w_r must be of the form

$$w_r = w_1(\phi) - \frac{Kx^2}{2} \cos \phi \tag{D10}$$

where $w_1(\phi)$ is an arbitrary function of ϕ only. Since $\sigma_\phi = M_\phi = 0$ at $\phi = 0$ and $\phi = \theta$, it can be shown from the equations of equilibrium that $\sigma_\phi = M_\phi = 0$ everywhere in this element. This information provides two relations from which expressions for $v_1(\phi)$ and $w_1(\phi)$ can be obtained. By using $\sigma_\phi = 0$ and the stress-strain relations for plane stress, there is obtained

$$\epsilon_\phi + \mu_c \epsilon_x = 0 \tag{D11}$$

and substituting for ϵ_ϕ and ϵ_x from equations (D5) and (D7), respectively, yields

$$\frac{1}{r_1}\frac{\partial v}{\partial \phi} - \frac{w_r}{r_1} - \mu_c K\left(e_1 + r_1 \cos \phi\right) = 0 \tag{D12}$$

Substituting the formulas for v and w_r from equations (D9) and (D10), respectively, into equation (D12) gives the first relation:

$$\frac{1}{r_1}\frac{\partial v_1}{\partial \phi} - \frac{w_1}{r_1} - \mu_c K\left(e_1 + r_1 \cos \phi\right) = 0 \tag{D13}$$

The second relation is obtained from $M_\phi = 0$ and from the moment-curvature relation

$$M_\phi = -D_c\left(\chi_\phi + \mu_c \chi_x\right) = 0 \tag{D14}$$

where

$$\chi_\phi = \frac{1}{r_1^2}\left(\frac{\partial v}{\partial \phi} + \frac{\partial^2 w_r}{\partial \phi^2}\right) \tag{D15}$$

$$\chi_x = \frac{\partial^2 w_r}{\partial x^2} \tag{D16}$$

Substituting equations (D15) and (D16) into equation (D14) gives

$$\frac{1}{r_1^2}\left(\frac{\partial v}{\partial \phi} + \frac{\partial^2 w_r}{\partial \phi^2}\right) = -\mu_c \frac{\partial^2 w_r}{\partial x^2} \tag{D17}$$

Again using equations (D9) and (D10) for v and w_r, respectively, yields the second relation:

$$\frac{1}{r_1^2}\left(\frac{\partial v_1}{\partial \phi} - \frac{Kx^2}{2}\cos \phi + \frac{\partial^2 w_1}{\partial \phi^2} + \frac{Kx^2}{2}\cos \phi\right) = \mu_c K \cos \phi \tag{D18}$$

Substituting the formula for $\frac{\partial v_1}{\partial \phi}$ from equation (D13) into equation (D18) gives

$$\frac{1}{r_1^2}\left[w_1 + \mu_c r_1 K\left(e_1 + r_1 \cos \phi\right) + \frac{\partial^2 w_1}{\partial \phi^2}\right] = \mu_c K \cos \phi \tag{D19}$$

or

$$\frac{\partial^2 w_1}{\partial \phi^2} + w_1 = -\mu_c r_1 K e_1 \tag{D20}$$

When equation (D20) is solved for w_1 and the result is substituted into equation (D10), the following equation results:

$$w_r = c_1 \sin \phi + c_2 \cos \phi - \mu_c r_1 K e_1 - \frac{Kx^2}{2} \cos \phi \tag{D21}$$

Similarly, using the solution to equation (D20) in conjunction with equations (D13) and (D9) yields

$$v = -c_1 \cos \phi + c_2 \sin \phi + \mu_c K r_1^2 \sin \phi - \frac{Kx^2}{2} \sin \phi + c_3 \tag{D22}$$

where c_1, c_2, and c_3 are arbitrary constants representing rigid-body displacements in the $x = 0$ plane. The quantities of interest in this analysis are the relative rotation of one end of element BC with respect to the other end in the $x = 0$ plane and the extension of the element in the y-direction in the $x = 0$ plane. These quantities can be obtained by ignoring rigid-body displacements. By setting $c_1 = c_2 = c_3 = x = 0$ in equations (D21) and (D22), it can be seen that there is no relative rotation of the ends of the element; that is, $\left.\frac{\partial w_r}{\partial \phi}\right|_{x=0} = 0$. The extension of the element in the y-direction is

$$\delta_2 = -(\sin \theta) w_r \Big|_{\substack{\phi=\theta \\ x=0}} + (\cos \theta) v \Big|_{\substack{\phi=\theta \\ x=0}} \tag{D23}$$

or

$$\delta_2 = \mu_c r_1 K e_1 \sin \theta + \mu_c K r_1^2 \sin \theta \cos \theta \tag{D24}$$

Element CD.- The axial strain in element CD is given by

$$\epsilon_x = Kz \tag{D25}$$

By considering the in-plane stress in the ξ-direction to be zero $(\sigma_\xi = 0)$ and by using the stress-strain relations for plane stress, there results

$$\epsilon_\xi = -\mu_c K z \tag{D26}$$

The total elongation in the ξ-direction from point C to point D is given by

$$\delta_\xi = \int_C^D \epsilon_\xi \, d\xi \tag{D27}$$

The extension in the y-direction is given by

$$\delta_3 = \delta_\xi \cos \theta \tag{D28}$$

or

$$\delta_3 = \frac{\mu_c K}{2} \cot \theta \left[\left(e_1 + r_1 \cos \theta \right)^2 - \left(e_2 + r_2 \cos \theta \right)^2 \right] \tag{D29}$$

Element DE.- The equations for v and w_r for the lower arc (element DE) are similar to those of the upper arc (element BC). The only differences are the substitutions of $-e_2$ for e_1 and r_2 for r_1. Angle ϕ is measured from the same reference line as for the case of the upper arc. Displacement w_r is positive toward the center of curvature of element DE. When rigid-body displacements are ignored,

$$w_r = \mu_c r_2 K e_2 - \frac{Kx^2}{2} \cos \phi \tag{D30}$$

$$v = \mu_c K r_2^2 \sin \phi - \frac{Kx^2}{2} \sin \phi \tag{D31}$$

As before, the relative rotations of the ends of the element are zero. The extension in the y-direction is given by

$$\delta_4 = -(\sin \theta) w_r \Big|_{\substack{\phi=\theta+\pi \\ x=0}} + (\cos \theta) v \Big|_{\substack{\phi=\theta+\pi \\ x=0}} \tag{D32}$$

or

$$\delta_4 = -\mu_c r_2 K e_2 \sin \theta - \mu_c K r_2^2 \sin \theta \cos \theta \tag{D33}$$

Element EF.- The axial strain for element EF is given by

$$\epsilon_x = K\left(e_2 + r_2 \right) \tag{D34}$$

If σ_y is considered to be zero,

$$\epsilon_y = -\mu_c K \left(e_2 + r_2 \right) \tag{D35}$$

The extension δ_5 of element EF is then given by

$$\delta_5 = -\mu_c Kg\left(e_2 + r_2\right) \tag{D36}$$

Analysis of Redundant Loads and Moments

In order for the corrugation and plate to have equal slopes and extensions at the weld line, equal and opposite redundant moments M and loads P act at the weld line. The deformations caused by these loadings are considered to be independent of the deformations caused by the linear strain distribution ϵ_x. The extension of the corrugation in the y-direction caused by moments M and loads P is given by $\frac{\partial U}{\partial P}$, where U is the strain energy of the corrugation due to bending. An expression for $\frac{\partial U}{\partial P}$ is given by equation (B10).

The total extension of the corrugation δ_c is given by

$$\delta_c = \sum_{n=1}^{5} \delta_n + \frac{\partial U}{\partial P} \tag{D37}$$

The extension of the plate δ_p is given by

$$\delta_p = \mu_p Kb\left(\bar{y} - \frac{t_p}{2}\right) \tag{D38}$$

Equating the extensions of the corrugation and plate at the weld line gives

$$\sum_{n=1}^{6} \delta_n + \frac{\partial U}{\partial P} = 0 \tag{D39}$$

where

$$\delta_6 = -\delta_p = -\mu_p Kb\left(\bar{y} - \frac{t_p}{2}\right) \tag{D40}$$

If, in equation (B10), M_c is replaced by M then $\frac{\partial U}{\partial P}$ can be expressed as a linear combination of M and P as follows:

$$\frac{\partial U}{\partial P} = \frac{1}{D_c}(\Lambda M + \Phi P) \tag{D41}$$

where $-\Lambda$ is the numerator of H and Φ is the denominator of H. (See eq. (B12).)

Let

$$\sum_{n=1}^{6} \delta_n = K\Sigma \tag{D42}$$

where

$$\Sigma = i\mu_c(e_1 + r_1) - g\mu_c(e_2 + r_2) + \mu_c r_1 e_1 \sin\theta + \mu_c r_1^2 \sin\theta\cos\theta + \frac{\mu_c \cot\theta}{2}\left[\left(e_1 + r_1\cos\theta\right)^2 - \left(e_2 + r_2\cos\theta\right)^2\right] - \mu_c r_2 e_2 \sin\theta - \mu_c r_2^2 \sin\theta\cos\theta - \mu_p b\left(\bar{y} - \frac{t_p}{2}\right) \tag{D43}$$

Upon substitution of equations (D41) and (D42) into equation (D39), the following equation is obtained:

$$K\Sigma = -\frac{1}{D_c}(\Lambda M + \Phi P) \tag{D44}$$

or

$$P = -\frac{D_c K\Sigma + \Lambda M}{\Phi} \tag{D45}$$

Since $\frac{\Lambda}{\Phi} = -H$, equation (D45) becomes

$$P = -\frac{D_c K\Sigma}{\Phi} + HM \tag{D46}$$

Inasmuch as the deformation caused by the linear strain distribution due to M_x makes no contribution to the slope, the slope of the corrugation at the weld line (relative to the slope at the center line of the cell) is given by $-\frac{\partial U}{\partial M}$ where a counterclockwise rotation is considered positive. An expression for $\frac{\partial U}{\partial M}$ is given by equation (B9) by replacing M_c by M. The slope of the plate at the weld line is given by $\frac{Mb}{D_p}$. Equating the slopes of the corrugation and plate at the weld line gives

$$\frac{\partial U}{\partial M} = -\frac{Mb}{D_p} \tag{D47}$$

From equation (B9), $\frac{\partial U}{\partial M}$ can be expressed as a linear combination of M and P as follows:

$$\frac{\partial U}{\partial M} = \frac{1}{D_c}(\Omega M + \Lambda P) \tag{D48}$$

where

$$\Omega = i + \theta(r_1 + r_2) + k + g \tag{D49}$$

Substituting the formulas for P and $\frac{\partial U}{\partial M}$ from equation (D46) and equation (D47), respectively, into equation (D48) yields

$$\frac{1}{D_c}\left[\Omega M + \Lambda\left(-\frac{D_c K \Sigma}{\Phi} + HM\right)\right] = -\frac{Mb}{D_p} \tag{D50}$$

Solving equation (D50) for $\frac{M}{KD_p}$ gives

$$\frac{M}{KD_p} = \frac{\Lambda\Sigma/\Phi}{\frac{D_p}{D_c}(\Omega + \Lambda H) + b} \tag{D51}$$

Equation (D51) can be simplified by noting that $\frac{\Lambda}{\Phi} = -H$ and from equation (B14) $\Omega + \Lambda H = X$. Since $\frac{M}{KD_p}$ is the ratio of anticlastic to primary curvature, equation (D51) determines μ_x if the panel is of the single-weld-line type. For the purpose of distinguishing this type from a double-weld-line type, the Poisson's ratio given by equation (D51) is designated μ_{x1}; that is,

$$\mu_{x1} = \frac{-H\Sigma}{\frac{D_p}{D_c} X + b} \tag{D52}$$

where H, Σ, and X are given by equations (B12), (D43), and (B14), respectively.

If the panel is constructed with a double weld line, the segment between weld lines must be considered. (See fig. 2.) The extension of one-half the cover plate between weld lines is given by

$$\mu_p K a\left(e_1 + r_1 + \frac{t_p + t_c}{2}\right) \tag{D53}$$

The extension of one-half the corrugation between weld lines is given by

$$\mu_c K a(e_1 + r_1) \tag{D54}$$

The curvature of this section is simply the difference between the extensions of the plate and the corrugation divided by the distance between the center lines of the plate and corrugation and by the distance a. The ratio of this curvature to K is designated μ_{x2} and is

$$\mu_{x2} = \mu_p + 2\frac{(\mu_p - \mu_c)(e_1 + r_1)}{t_p + t_c} \tag{D55}$$

The ratio of anticlastic curvature to primary curvature for the entire panel is then

$$\mu_x = \frac{b\mu_{x1} + a\mu_{x2}}{b + a} \tag{D56}$$

where μ_{x1} and μ_{x2} are given by equations (D52) and (D55), and a and b are dimensions shown in figure 2. By using the reciprocity theorem for elastic structures, μ_y is obtained as follows:

$$\mu_y = \mu_x \frac{D_y}{D_x} \tag{D57}$$

For a corrugation-stiffened panel, the ratio of D_y to D_x is usually very small so that μ_y is very small. Although μ_x may not be small compared with unity, the product $\mu_x\mu_y$ is usually small compared with unity. For example, the product $\mu_x\mu_y$ is less than 3×10^{-5} for the test panels considered in this report (see table II).

REFERENCES

1. Libove, Charles, and Hubka, Ralph E.: Elastic Constants for Corrugated-Core Sandwich Plates. NACA TN 2289, 1951.

2. Stein, Manuel, and Mayers, J.: A Small-Deflection Theory for Curved Sandwich Plates. NACA Rep. 1008, 1951. (Supersedes NACA TN 2017.)

3. Libove, Charles, and Batdorf, S. B.: A General Small-Deflection Theory for Flat Sandwich Plates. NACA Rep. 899, 1948. (Supersedes NACA TN 1526.)

4. Garofalo, F., Malenock, P. R., and Smith, G. V.: The Influence of Temperature on the Elastic Constants of Some Commercial Steels. Symposium on Determination of Elastic Constants, Special Tech. Pub. No. 129, ASTM, c.1952, pp. 10-27.

5. Anon.: Inconel "X" - A High Strength, High Temperature Alloy, Data and Information. Dev. and Res. Div., The Int. Nickel Co., Inc., Jan. 1949, p. 10.

6. Zender, George W., and Brooks, William A., Jr.: An Approximate Method of Calculating the Deformations of Wings Having Swept, M or W, Λ, and Swept-Tip Plan Forms. NACA TN 2978, 1953.

7. Herr, Robert W.: A Wide-Frequency-Range Air-Jet Shaker. NACA TN 4060, 1957.

8. Young, Dana, and Felgar, Robert P., Jr.: Tables of Characteristic Functions Representing Normal Modes of Vibration of a Beam. Univ. of Texas Pub. No. 4913, Eng. Res. Ser. No. 44, Bur. Eng. Res., July 1, 1949.

9. Popov, E. P.: Mechanics of Materials. Prentice-Hall, Inc., c.1952, p. 115.

10. Kuhn, Paul: Stresses in Aircraft and Shell Structures. McGraw-Hill Book Co., Inc., 1956, pp. 12-14.

NASA-Langley, 1964 L-1863